Carcinogenesis vol.33 no.11 pp.2162–2171, 2012
doi:10.1093/carcin/bgs240
Advance Access publication July 20, 2012

ROS-independent JNK activation and multisite phosphorylation of Bcl-2 link diallyl tetrasulfide-induced mitotic arrest to apoptosis

Mareike Kelkel[1,†], Claudia Cerella[1,†], Fabienne Mack[1], Thomas Schneider[3], Claus Jacob[3], Marc Schumacher[1], Mario Dicato[1] and Marc Diederich[1,2,*]

[1]Laboratoire de Biologie Moléculaire et Cellulaire du Cancer, Fondation de Recherche Cancer et Sang, Hôpital Kirchberg, 9, rue Edward Steichen, L-2540 Luxembourg, Luxembourg; [2]College of Pharmacy, Seoul National University, Seoul 151-742, South Korea and [3]Division of Bioorganic Chemistry, School of Pharmacy, Saarland University, D-66123 Saarbrücken, Germany

*To whom correspondence should be addressed. Tel: +352 2468 4040; Fax: +352 2468 4060; Email: marc.diederich@lbmcc.lu

Garlic-derived organosulfur compounds including diallyl polysulfides are well known for various health-beneficial properties and recent reports even point to a potential role of diallyl polysulfides as chemopreventive and therapeutic agents in cancer treatment due to their selective antiproliferative effects. In this respect, diallyl tri- and tetrasulfide are reported as strong inducers of an early mitotic arrest and subsequent apoptosis, but the underlying molecular mechanisms and the link between these two events are not yet fully elucidated. Our data revealed that diallyl tetrasulfide acts independently of reactive oxygen species and tubulin represents one of its major cellular targets. Tubulin depolymerization prevents the formation of normal spindle microtubules, thereby leading to G2/M arrest. Here, we provide evidence that c-jun N-terminal kinase, which is activated early in response to diallyl tetrasulfide treatment, mediates multisite phosphorylation and subsequent proteolysis of the anti-apoptotic protein B-cell lymphoma 2. As the latter event occurs concomitantly with the onset of apoptosis and the chemical c-jun N-terminal kinase inhibitor SP600125 not only prevented B-cell lymphoma 2 phosphorylation and proteolysis but also apoptosis following diallyl tetrasulfide treatment, we suggest that these c-jun N-terminal kinase-mediated modulations of B-cell lymphoma 2 represent the missing link connecting early microtubule inactivation to the induction of apoptosis.

Introduction

Many plants contain a specific set of natural compounds with various health beneficial properties including anticancer activities. As these promising chemopreventive and chemotherapeutic properties are rarely associated with harmful side effects, natural compounds gain more and more importance in cancer research. Organosulfur compounds (OSCs), ubiquitous in garlic and other *Allium* plants, possess chemopreventive properties (1,2) and are mainly responsible for the inverse correlation between garlic consumption and incidence of different cancers observed in epidemiological studies (3–6). *In vivo* studies provided evidence that diallyl sulfides (DASs), one class of garlic OSCs, effectively prevent chemically induced carcinogenesis in animal models, for review see (5,7,8).

We and others demonstrated that the anticancer activity of DASs is associated with the number of sulfur atoms (9–12). Our previous data revealed that the most potent compound diallyl tetrasulfide (DAS4) induces an early mitotic arrest in different cancer cell models (10,13,14). Depending on the cell line, this cell cycle dysfunction gives rise to apoptotic cell death (10,14).

Polysulfides are often suggested to act via reactive oxygen species (ROS) induction and antioxidants such as *N*-acetylcysteine (NAC) were shown to counteract the biological activities of these compounds (12,15–20). ROS accumulation disturbs the cellular redox balance and causes oxidative stress. The excess of highly reactive radicals interferes with cellular signaling pathways by attacking cellular macromolecules including proteins and DNA (21). Other studies reported that OSCs directly modify protein sulfhydryl groups under generation of mixed disulfides (22–24).

Previously, we noted that in U937 cells, DAS4-induced mitotic arrest is followed by modulation of B-cell lymphoma 2 (Bcl-2) family members. In this regard, proteolysis of the anti-apoptotic protein Bcl-2 was detected concomitant with the onset of apoptosis (10). The Bcl-2 protein family, consisting of pro- and anti-apoptotic members, plays a key role in the regulation of apoptosis. The most important anti-apoptotic member, Bcl-2, whose activity may be modulated by different phosphorylation events, acts at the level of the mitochondria via sequestration of Bcl-2-associated X protein (Bax), thereby abrogating its pro-apoptotic function (25). Bcl-2 function requires a rapid single-site phosphorylation at serine 70 (26–28) occurring during normal cell cycle progression at G2/M phase (26,28). However, during prolonged mitotic arrest caused by microtubule (MT) interacting agents, two supplementary phosphate groups are added to Bcl-2 (27–29). This multisite phosphorylation proceeds delayed (30) and correlates with a loss of function favoring apoptotic cell death (30,31).

In our system, ROS are not implicated in the cellular response to DAS4. We identified tubulin as the major direct target protein of DAS4 and the resulting microtubule disassembly as the main trigger for mitotic arrest. Interestingly, our data indicate that Bcl-2 undergoes an early multisite phosphorylation in response to DAS4 that timely precedes its proteolysis and concomitant apoptosis. c-Jun N-terminal kinase (JNK), which is activated early upon DAS4 treatment, mediates this posttranslational modification, subsequent Bcl-2 proteolysis and apoptosis. We therefore conclude that JNK-mediated multisite phosphorylation of Bcl-2 represents the missing link between early mitotic arrest and the onset of apoptosis in response to DAS4 treatment.

Materials and methods

Cell culture

U937 cells (human histiocytic lymphoma, DSMZ) were cultured in RPMI 1640 medium containing ultraglutamine 1 (Bio-Whittaker, Verviers, Belgium) supplemented with 10% (v/v) of fetal calf serum (Lonza, Verviers, Belgium), 1% (v/v) of antibiotic/antimycotic (Lonza, Verviers, Belgium) at 37°C and 5% CO_2. All experiments were performed in culture medium containing 0.1% of fetal calf serum.

Reagents

DAS, diallyl disulfide (DAS2), allylmercaptan (AM) and 1,9-decadiene were purchased from Sigma-Aldrich-Fluka (Darmstadt, Germany). DAS and 1,9-decadiene were used without further purification, AM and DAS2 were purified by distillation under reduced pressure. Diallyl trisulfide (DAS3), DAS4 and the propyl analogues DPS3 and

Abbreviations: AM, allylmercaptan; ASK-1, apoptosis signal-regulating kinase 1; Bak, Bcl-2 homologous antagonistic killer; Bax, Bcl-2-associated X protein; Bcl-2, B-cell lymphoma 2; BSA, bovine serum albumin; CMFDA, 5-chloromethylfluorescein diacetate; DAS, diallyl sulfide; DAS2, diallyl disulfide; DAS3, diallyl trisulfide; DAS4, diallyl tetrasulfide; DMSO, dimethyl sulfoxide; ERK, extracellular-regulated kinase; GSH, reduced glutathione; GSSG, oxidized glutathione; H_2O_2, hydrogen peroxide; H3P, phospho-Histone H3 (Ser10); JNK, c-Jun N-terminal kinase; MAPK, mitogen-activated protein kinase; MT, microtubules; NAC, *n*-acetylcysteine; OSCs, organosulfur compounds; ROS, reactive oxygen species.

†These authors contributed equally to this work.

DPS4 were synthesized from the Jacob group at the University of the Saarland according to procedures of Derbesy *et al.* (32) and Milligan *et al.* (33,34). NAC (sterile water; 10 mM) and Trolox (ethanol; 1 mM) were added, respectively, 48 and 1 h before DAS4 treatment. Both antioxidants were purchased from Sigma-Aldrich (Bornem, Belgium). SP600125 (Calbiochem, Leuven, Belgium), PD98059 and SB203580 (Promega, Leiden, Netherlands) were dissolved in dimethyl sulfoxide (DMSO) and added 30 min before at a concentration of 25 or 20 µM (extracellular-regulated kinase [ERK] and p38).

Paclitaxel (Hospira Deutschland GMBH, Munich, Germany) was added at a concentration of 175 nm for 8 h.

Detection of nuclear morphology (Hoechst staining)

Percentage of apoptotic and early-blocked mitotic cells was quantified by fluorescence microscopic analysis (Leica-DM IRB microscope, Lecuit, Luxembourg) after staining with 1 µg/ml Hoechst 33342 (Sigma, Bornem, Belgium) (35,36).

Total extraction of cellular proteins and western blot analysis

Whole cell extracts were prepared as described (35,36). Cells were dissolved in M-PER® (Mammalian Protein Extraction Reagent; Pierce, Erembodegem, Belgium) supplemented by a protease inhibitor cocktail (Complete®, Roche), 1 µM phenylmethylsulfonyl fluoride (Sigma), phosphatase inhibitors: Phospho-Stop® (Roche; Prophac SARL, Howald, Luxembourg), 5 mM sodium fluoride and 10 mM sodium *ortho*-vanadate (Sigma-Aldrich, Bornem, Belgium)). 20–40 µg proteins were separated by sodium dodecyl sulfate–polyacrylamide gel electrophoresis (12%) and transferred to polyvinylidene difluoride membranes (GE Healthcare, Roosendaal, The Netherlands). Beta-actin served as loading control. Anti-beta-actin (Sigma), anti-Bcl-2 (Calbiochem), anti-phospho-Bcl-2 (Ser70), anti-phospho-JNK (Cell Signaling, Leiden, The Netherlands) and anti-JNK (Santa Cruz Biotechnology, Boechout, Belgium) were used as primary antibodies (0.5–1 µg/ml) and incubated for 1 h or overnight. Specific immunoreactive proteins upon incubation with specific horseradish peroxidase–conjugated secondary antibodies [Santa Cruz Biotechnology or BD Pharmingen (Erembodegem, Belgium)] were visualized by chemiluminescence using the ECL Plus Western Blotting Detection System Kit® (GE Healthcare, Roosendaal, The Netherlands).

Indirect immunofluorescence

Cells were fixed and permeabilized using the BD Cytofix/Cytoperm Kit® (Becton Dickinson, Erembodegem, Belgium). Incubations with the following primary antibodies (10 µg/ml; 1 h at room temperature) were performed: anti-phospho-Histone H3 (Ser10) (rabbit, polyclonal; Upstate Biotechnology, Lake Placid, NY, USA); anti-alpha-tubulin (mouse, monoclonal; Calbiochem). After incubation with the corresponding secondary antibody (8 µg/ml, room temperature for 30 min) on a shaking platform (rabbit Alexafluor 568 or mouse Alexafluor 488; Invitrogen/Molecular Probes, Merelbeke, Belgium), cells were counterstained with Hoechst 33342 and monitored by fluorescence microscopy (Olympus, Hamburg, Germany). The images were analyzed/elaborated using Cell^M software (Olympus Soft Images Solutions GmbH, Germany).

Fluorescence-activated cell-sorting analysis

Cell cycle. Cell cycle was analyzed according to standard procedures. In brief, cells were fixed with an ethanol solution (70% v/v) and DNA was treated with RNase A (100 µg/ml; Roche, Luxembourg) and propidium iodide (1 µg/ml; Sigma-Aldrich, Bornem, Belgium) in phosphate-buffered saline.

ROS detection. DAS4/DMSO-treated cells were stained for 20 min with 10 nM ROS-detection agent dichlorodihydrofluorescein diacetate (H_2DCFDA) at 37°C. 50 µM hydrogen peroxide (H_2O_2)-induced generation of fluorescent 2′,7′-dichlorofluorescein (DCF) served as positive control.

Mitochondrial membrane potential. Apoptosis was further estimated by incubating 1×10^6 cells at 37°C for 20 min with 50 nM MitoTracker® Red (Molecular Probes/Invitrogen).

Incubations were followed by flow cytometry (fluorescence-activated cell sorting calibur, BD Biosciences, San José, CA, USA). Events were recorded statistically (10 000 events/sample) using CellQuest software (http://www.bdbiosciences.com/features/products/display_product.php?keyID=92). Data were further analyzed using FlowJo 8.8.7 software (Tree Star Inc).

In vitro *tubulin polymerization assay*

Tubulin polymerization was measured in presence and absence of test compound by using the Tubulin Polymerization Assay Kit (Cytoskeleton, Boechout, Belgium) according to manufacturer's instructions. Briefly, 5 µl of each test compound (10× solution) were added in triplets in wells of a prewarmed, black 96-well plate. After addition of 50 µl of ice-cold porcine tubulin solution, the fluorescence emission was detected at 450 nm at 37°C using a Spectra Max Gemini EM fluorescence microplate reader (Molecular Devices, Inc. Sunnyvale, CA, USA) and followed during 1 h with one reading per minute. Paclitaxel (30 µM)and $CaCl_2$ (5 mM) served as 10× enhancer and inhibitor control solutions of tubulin polymerization, respectively, according to manufacturer's instruction.

Reduced glutathione assay

CellTracker™ Green. CellTracker™ Green [5-chloromethylfluorescein diacetate (CMFDA); Molecular Probes] served as fluorescent probe for the indirect determination of reduced glutathione (GSH) content. U937 cells (5×10^5 cells/ml in medium) were treated for 1 or 2 h with H_2O_2 (positive control), 5 and 10 µM DAS4 or equal volume of vehicle. Then, the cells were incubated at 37°C for 20 min with 10 nM CMFDA. Fluorescence was determined by fluorometric analysis (Ex. 485 nm, Em. 538 nm).

GSH/GSSG-GloTM assay. GSH/GSSG ratio was determined using GSH/GSSG-Glo™ Assay (Promega). GSH depletion was achieved by pretreating cells 24 h with L-buthionine sulphoximine (BSO) (1 mM). U937 cells were resuspended at a concentration of 1×10^6/ml in prewarmed Hank's Buffered Salt Solution (HBSS). About 20 µl of the cell suspensions were transferred into wells of a 96-well plate; 5 µl of 5× concentrated test compound/vehicle were added to each well. HBSS alone served as no-cell control. After incubation for 2 h at 37°C, total GSH/GSSG levels were determined by luminescence (integration time: 1 s/well).

Statistical analysis

Data are presented as mean of at least three independent experiments ± standard deviation. The Student *t*-test was used to determine statistically significant means. The level of significance was defined as $P < 0.01$ and $P < 0.001$ was considered highly significant.

Results

The effects of DAS4 on mitotic arrest and apoptosis are ROS-independent in U937 cells

We have shown previously that DAS4 induces the arrest of U937 cells in early mitosis, peaking at 8 h of incubation, followed by the induction of apoptosis (10). The block is marked by particular alterations, including the accumulation of H3P (Ser 10) (10). The biological effects of sulfur compounds have been attributed to the elicitation of oxidative stress; ROS generation has been frequently postulated as causative event (19,20,37).

We investigated ROS implication in our instance. Pretreatment with NAC, an anti-oxidant agent, which increases the intracellular glutathione (GSH) pool, widely used to prove pro-oxidant activities of DASs (17,23,38), completely inhibited histone H3 phosphorylation (Figure 1A). Trolox, an analogue of vitamin E acting specifically as ROS scavenger did not exert any modulatory effect (Figure 1A). Cell cycle (Figure 1B) and microscopic analysis of Hoechst-stained nuclei (Figure 1C) confirmed these differential effects on G2/M accumulation and apoptosis prevention (10) suggesting that ROS do not play causative role in the DAS4 response.

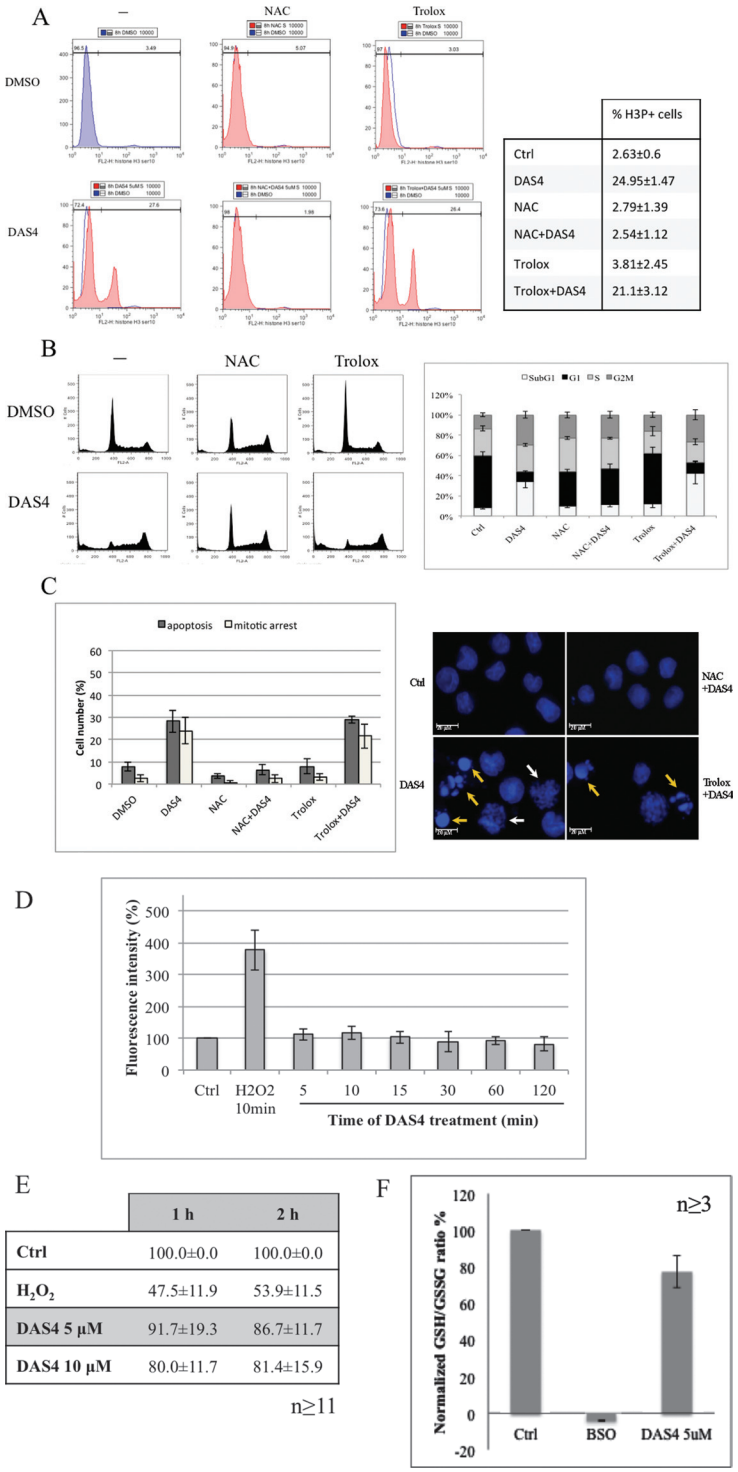

	% H3P+ cells
Ctrl	2.63±0.6
DAS4	24.95±1.47
NAC	2.79±1.39
NAC+DAS4	2.54±1.12
Trolox	3.81±2.45
Trolox+DAS4	21.1±3.12

	1 h	2 h
Ctrl	100.0±0.0	100.0±0.0
H_2O_2	47.5±11.9	53.9±11.5
DAS4 5 µM	91.7±19.3	86.7±11.7
DAS4 10 µM	80.0±11.7	81.4±15.9

n≥11

Fig. 1. The effects of DAS4 on mitotic arrest and apoptosis are ROS-independent in U937 cells. U937 cells were pretreated with the antioxidants NAC (10 mM, 48 h) or Trolox (1 mM, 1 h) and then treated with either 5 µM DAS4 or DMSO for 8 h in order to reach a peak of cells in G2/M arrest. (**A**) Immunostaining was performed using an anti-phospho-histone H3 (Ser10) antibody. H3P-positive cells were quantified by fluorescence-activated cell-sorting analysis and the fraction of positive cells ($n = 3$ ±SD) is listed in the table for each treatment. (**B**) Cell cycle was analyzed in parallel by flow cytometry upon PI staining. Results are presented both as a representative histogram and a chart showing the cell-cycle distribution ($n = 3$ ±SD) (**C**) By microscopic analysis of Hoechst-stained nuclei, the percentage of apoptotic cells (yellow arrows) and cells in mitosis (displaying prometaphase-like pattern; white arrows) was calculated by counting ×3 100 cells. The quantification is given in a chart format ($n = 4$ ±SD). For quantification of ROS, U937 cells were treated with DAS4 (5 µM) or vehicle DMSO. Treated and control cells were incubated with the peroxide specific dye dichlorodihydrofluorescein diacetate (10 nM) for 20 min at 37°C and 5% CO_2. After indicated time points, the fluorescence signal was quantified via flow cytometry. H_2O_2-treated cells (50 µM, 10 min) served as positive control. (**D**) Data are depicted as mean of the fluorescence intensity, normalized to the solvent control ±SD, ($n = 4$). (**E**) Intracellular thiol groups were quantified using fluorescent dye CellTracker™ Green CMFDA. H_2O_2 served as negative control. CMFDA was added at an end concentration of 10 nM after 1 h or 2 h incubation time with 5 µM DAS4/solvent and after 20 min of incubation. (**F**) GSH/GSSG ratio of U937 cells was measured upon 24 h L-buthionine sulphoximine pretreatment (1 mM) and treatment with 5 µM DAS4 or solvent for 2 h using GSH/GSSG-Glo™ Assay (Promega).GSH/GSSG ratio was normalized and the values of three independent experiments are given in % ±SD.

To adduce further evidence, we monitored ROS accumulation in DAS4-treated/untreated cells over the time with the fluorescent ROS indicator dichlorodihydrofluorescein diacetate (H_2DCFDA). The analysis included the detection of ROS since very early incubation times, up to 2 h, as ROS accumulation is expected to occur quickly (Figure 1D). No significant change in ROS staining was observable at any time point in contrast to 10-min treatment with 50 µM H_2O_2 (Figure 1D). We further excluded a very fast peak of ROS production immediately upon the addition of DAS4, as well as after later time points up to 24 h of treatment (data not shown).

However, the results with NAC imply that the redox state is affected by DAS4. GSH is the most abundant nonprotein thiol playing an important role in the cellular antioxidant defense and controls the cellular redox state by directly interacting with ROS or indirectly via detoxification enzymes (39). By using CellTracker™ Green CMFDA, indirect fluorescent determination of GSH content revealed that DAS4 reduced GSH levels: from 8.3% to 13.3% reduction after 1 h and 2 h, respectively, with treatment at 5 µM, to 20 and 18.6% after 1 h and 2 h with 10 µM DAS4 (Figure 1E). The direct estimation of GSH/GSSG levels by fluorometric assay (see 'Materials and methods') confirmed these findings: the addition of 5 µM DAS4 to U937 cells for 2 h decreased the ratio by 22.7 ± 8.7% (Figure 1F). Altogether these data indicate that the biological effects of DAS4 are mediated by changes in cell redox state without ROS implication.

In vitro *inhibition of tubulin polymerization by DAS4 depends on its sulfur atoms*

We considered tubulin as a possible cellular target of DAS4. First, DAS4 does not induce DNA damage within the time of DAS4 treatment leading to cell cycle arrest (40) (Supplementary Figure 1, available at *Carcinogenesis* Online). Second, this hypothesis is in line with previous findings regarding DAS3 (22). Third, changes in the microtubule dynamic lead to the activation of the mitotic spindle assembly checkpoint, which finally ends in a mitotic arrest if the spindle microtubules cannot be formed correctly (41). DAS4-treated U937 cells arrested G2/M (positive for H3P) concomitantly showed a dotted-like pattern of α-tubulin, as expected in the case of an aberrant accumulation of unpolymerized tubulin monomers (Figure 2A). To test the hypothesis that DAS4 might act as a tubulin-depolymerizing agent, we performed an *in vitro* tubulin turbidity assay. Incubation of a tubulin polymer stock with DAS4 (10 µM) significantly reduced the fluorescence signal compared with the DMSO control and the mitotic inhibitor paclitaxel indicating a substantial inhibition of tubulin polymerization (Figure 2B). Paclitaxel served as positive control as it acts by stabilizing microtubules. Conversely, $CaCl_2$, which rapidly depolymerizes microtubules *in vitro* (42), served as inhibitor control. 1,9-decadiene, a compound containing nonreactive carbon atoms instead of sulfur, had only a very mild effect on tubulin polymerization. Besides, AM, which contains a single sulfur in the form of a reduced –SH group (43), did not alter the tubulin polymerization appreciably. Finally, the tubulin depolymerizing activity correlated with the number of sulfur atoms of the tested diallyl polysulfides (Figure 2C): DAS4 exerted the strongest effect, followed by DAS3, whereas DAS2 and DAS only barely affected the tubulin polymerization. These findings strengthen the hypothesis that sulfur atoms mediate direct interaction with tubulin.

Thiol group within the cell-permeable NAC (or other intracellular small thiol molecules as GSH) may interfere with the highly reactive sulfur atoms of DAS4 under the formation of a mixed disulfide (9,43), thereby preventing interactions between the sulfur atoms of DAS4 and its cellular target(s). To test this, we co-incubated the tubulin polymer stock with 10 µM DAS4 and 10 mM NAC and observed that NAC completely restored the fluorescence values (Figure 2D), indicating its direct ability to counteract the DAS4-induced microtubule disassembly *in vitro*. Microscopic analysis of changes in the tubulin pattern in cells pre-treated with NAC or Trolox verified the results of the *in vitro* tubulin assay (Figure 2E). The consistent fraction of H3P-positive mitotic cells accumulating upon 8 h treatment with DAS4 never showed a mitotic spindle or normal microtubule structures—the same was observed for Trolox-pre-treated cells. Instead, after NAC pre-treatment, a striking small number of H3P-positive cells were found, and in accordance with the findings of the tubulin assay, these cells possessed normal spindle microtubules – a fact arguing for a protective role of NAC exclusively.

DAS4 induces JNK-dependent multisite phosphorylation of Bcl-2

Microtubule interacting agents cause a multisite phosphorylation of Bcl-2 (28); one of the residues implicated is serine 70. Whereas a single-site phosphorylation, occurring during normal cell-cycle progression at G2/M phase, has a prosurvival effect (26,28); multisite phosphorylation of Bcl-2 inactivates its anti-apoptotic function (28,31). DAS4 induces proteolysis of Bcl-2 concomitantly with the onset of apoptosis (10). Here we analyzed if early Bcl-2 phosphorylation may take place upon DAS4 treatment. Figure 3A shows the western blot kinetic analysis of the phosphorylation state of the Bcl-2 protein in presence of DAS4 over 24 h. Multiple upshifted bands were detectable as early as 0.5–1 h, with a maximum signal after 8 h [when the strongest accumulation in G2/M phase takes place (10)], to disappear after longer incubation with DAS4. An additional band corresponding to the cleaved form of Bcl-2 was detected in the samples of 16 and 24 h treatment, confirming previous results (10). The multisite phosphorylation involves serine 70: we detected phospho-Bcl-2 (Ser70) bands as early as 0.5 h after DAS4 treatment (Figure 3A). An upshifted band was observable as a sign of an ongoing further event of phosphorylation. The specific timing of Bcl-2 modulations suggests that the multisite phosphorylation of Bcl-2 is required for subsequent proteolysis of this anti-apoptotic protein.

JNK is implicated in multisite phosphorylation of Bcl-2; its activation was found to take place following tubulin alterations (44–48). Of importance, JNK activation has been observed in various cell models exposed to sulfur compounds (24,38,49). To elucidate a potential role of this kinase in the DAS4-induced multisite phosphorylation of the Bcl-2 protein, we assayed the status of JNK activation by western blotting (Figure 3B). JNK phosphorylation was visible starting from 0.5 h DAS4 treatment to peak between 1 and 4 h. The modulation pattern induced by DAS4 on JNK and Bcl-2 is similar to the one induced by MT-depolymerizing agents, that is, vincristine and vinblastine, on our cell model (Supplementary Figure 2, available at *Carcinogenesis* Online), thus indicating a common cellular response to DAS4 and known MT inhibitor agents.

The early activation of JNK, concomitant with the multisite phosphorylation of Bcl-2, is suggestive of a causative role of this kinase. Specific JNK inhibitor SP600125 almost completely prevented multisite phosphorylation of Bcl-2, thus confirming a role of JNK in Bcl-2 multisite phosphorylation (Figure 3C). In contrast, inhibitors against mitogen-activated protein kinase (MAPK)/ERK kinase I (PD98059) and p38MAPK (SB203580) showed only mildly or no effects on DAS4-induced multiple Bcl-2 phosphorylation. The analysis with the phospho-specific Bcl-2 (Ser70) antibody revealed that the effect produced by ERK inhibitor concerns the event of Bcl-2 phosphorylation occurring on other sites (Figure 3C, top panel). Combinational treatment with JNK/p38 or JNK/ERK inhibitors together with DAS4 further reduced the signal. Taking into account that impact of the pre-treatment with each couple of inhibitors alone, no further inhibition of multisite phosphorylation could be achieved by DAS4. From these data, we can conclude that JNK is the major kinase implicated in multisite phosphorylation of Bcl-2.

JNK is critical for Bcl-2 proteolysis and induction of the apoptotic program

Next, we investigated the effect of chemical kinase inhibitors on DAS4-induced apoptotic cell death. The protective potential of each inhibitor against apoptosis correlates with their inhibitory effect on multisite phosphorylation of Bcl-2 (see Figure 3C). Only JNK inhibitor significantly counteracted the apoptogenic potential of DAS4 (Figure 4A). PD98059 mildly affected apoptosis but the effect was enhanced after combinational treatment with SP600125. SB203580 did not have any impact. As Bcl-2 proteolysis occurs concomitantly with the onset of apoptosis (10) and JNK modulates

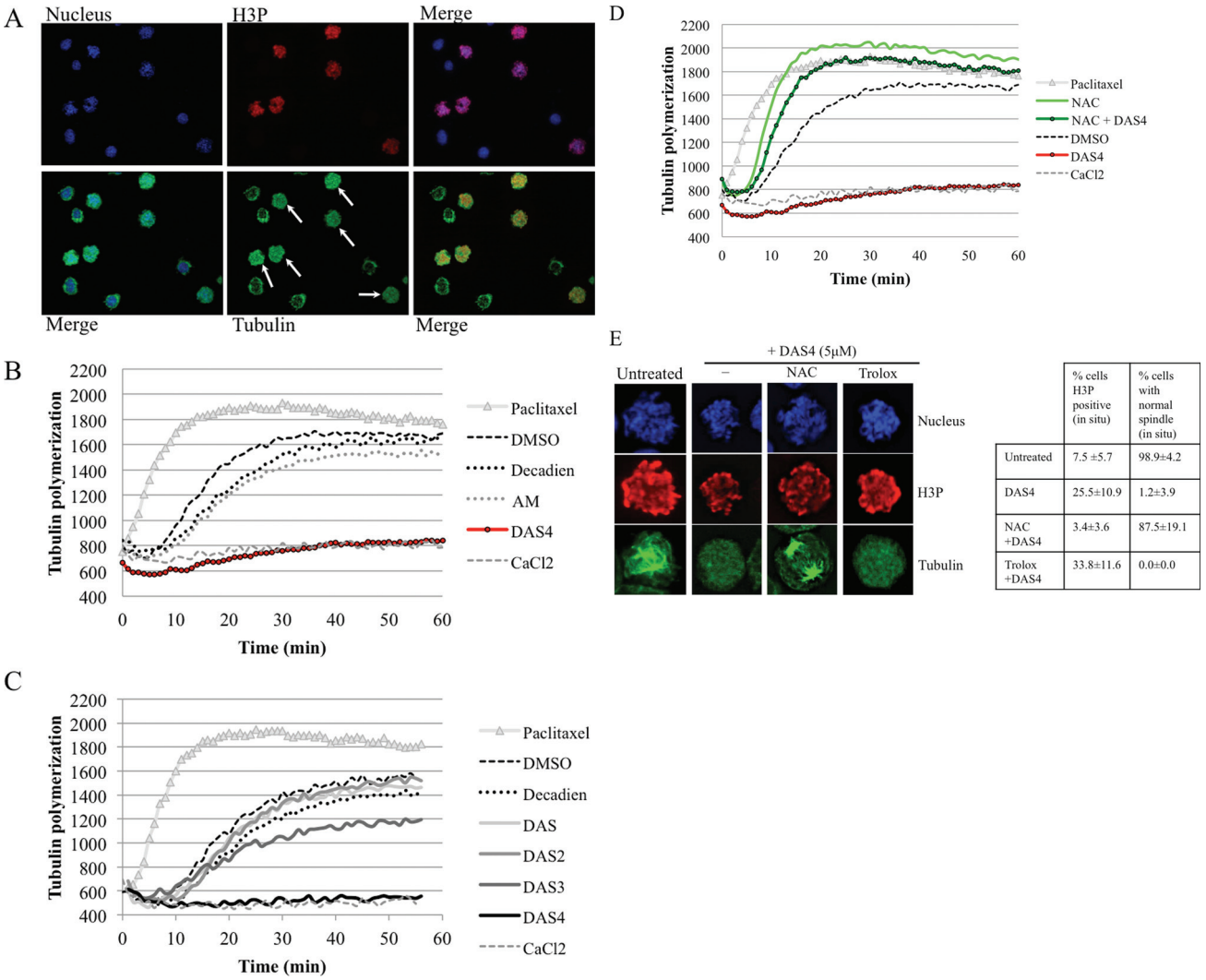

	% cells H3P positive (in situ)	% cells with normal spindle (in situ)
Untreated	7.5 ±5.7	98.9±4.2
DAS4	25.5±10.9	1.2±3.9
NAC +DAS4	3.4±3.6	87.5±19.1
Trolox +DAS4	33.8±11.6	0.0±0.0

Fig. 2. *In vitro* inhibition of tubulin polymerization by DAS4 depends on its sulfur atoms and is counteracted by NAC. (**A**) Phosphorylation of histone H3 as a marker of early mitosis/mitotic arrest was assessed in U937 cells after 8 h DAS4 treatment by immunostaining using an antibody specifically recognizing phosphorylation at Ser10. Cells were counterstained with Hoechst and anti-α-tubulin antibody in order to monitor nuclear morphology and the cytoskeleton, respectively. Arrows indicate H3P positive cells with an abnormal, dotted-like tubulin pattern lacking spindle MTs (**B**) Cell-free tubulin turbidity assay was performed to confirm the tubulin depolymerizing activity of DAS4 *in vitro*. A tubulin polymer stock was incubated with DAS4 (10 μM). Equal molarities of decadiene and AM served as negative control to demonstrate the importance of the sulfur atoms in DAS4. DMSO was added as vehicle control. Paclitaxel (3 μM) and $CaCl_2$ (500 μM) represent enhancer and inhibitor controls for the tubulin polymerization reaction, respectively. The fluorescence was monitored by a fluorometer (Ex. 360 nm; Em. 450 nm) over 60 min at 37°C to allow an optimal tubulin polymerization. (**C**) To assess the role of the number of sulfur atoms, the experiment was performed in parallel with DAS, DAS2 and DAS3. (**D**) A possible protective effect of NAC on DAS4-induced MT depolymerization was investigated by the *in vitro* tubulin turbidity assay as explained above. The tubulin polymer stock was incubated with DAS4 alone or in combination with NAC (10 mM). (**E**) To confirm the protection by NAC *in cellulo*, U937 cells were first pretreated with the antioxidants NAC (10 mM, 48 h) or Trolox (1 mM, 1 h). After subsequent incubation with DAS4 (5 μM) or an equivalent volume of DMSO for 8 h, the cells were immunostained with antibodies specifically recognizing phospho-histone H3 (Ser10) (H3P) and α-tubulin. Cells were counterstained with Hoechst to monitor the nuclear morphology. The tubulin pattern of H3P-positive cells was then assessed by fluorescence microscopy. The right panel presents the *in situ* quantification of H3P-positive cells, as well as the percentage of these cells with normal mitotic spindle MTs for each treatment (n = 3 ±SD).

the phosphorylation state of this anti-apoptotic protein, we investigated the effect of kinase inhibitors on Bcl-2 cleavage (Figure 4B). Again, ERK inhibitor mildly reduced the effect of DAS4, whereas p38 did not alter Bcl-2 proteolysis. The band intensity upon co-treatment with JNK inhibitor and DAS4 is comparable with that after DAS4 treatment. However, considering that already JNK inhibitor alone at the used concentration led to Bcl-2 cleavage, the result points to a rescuing effect of JNK and is in line with previous observations (42). To further evaluate the role of Bcl-2 in DAS4-induced apoptosis, we used as alternative strategy a small molecular Bcl-2 inhibitor (50,51) and verified its ability to modulate the effects of DAS4 on cell-cycle arrest and apoptosis induction (Supplementary Figure 3, available at *Carcinogenesis* Online). We witnessed that the Bcl-2 inhibitor per se affects cell viability but not the cell cycle in U937 cells that express high levels of Bcl-2. When combined to DAS4, no further modulation of the cell cycle was observed; in contrast, the percentage of apoptotic cells was consistently reduced compared with the sum of the apoptotic cells obtained by single treatments.

NAC prevented DAS4-induced JNK activation and multisite phosphorylation of Bcl-2

We have shown the differential ability of NAC versus Trolox to impact apoptosis induced by DAS4. Here, we verified any differential influence of these two agents on DAS4-dependent JNK activation and Bcl-2

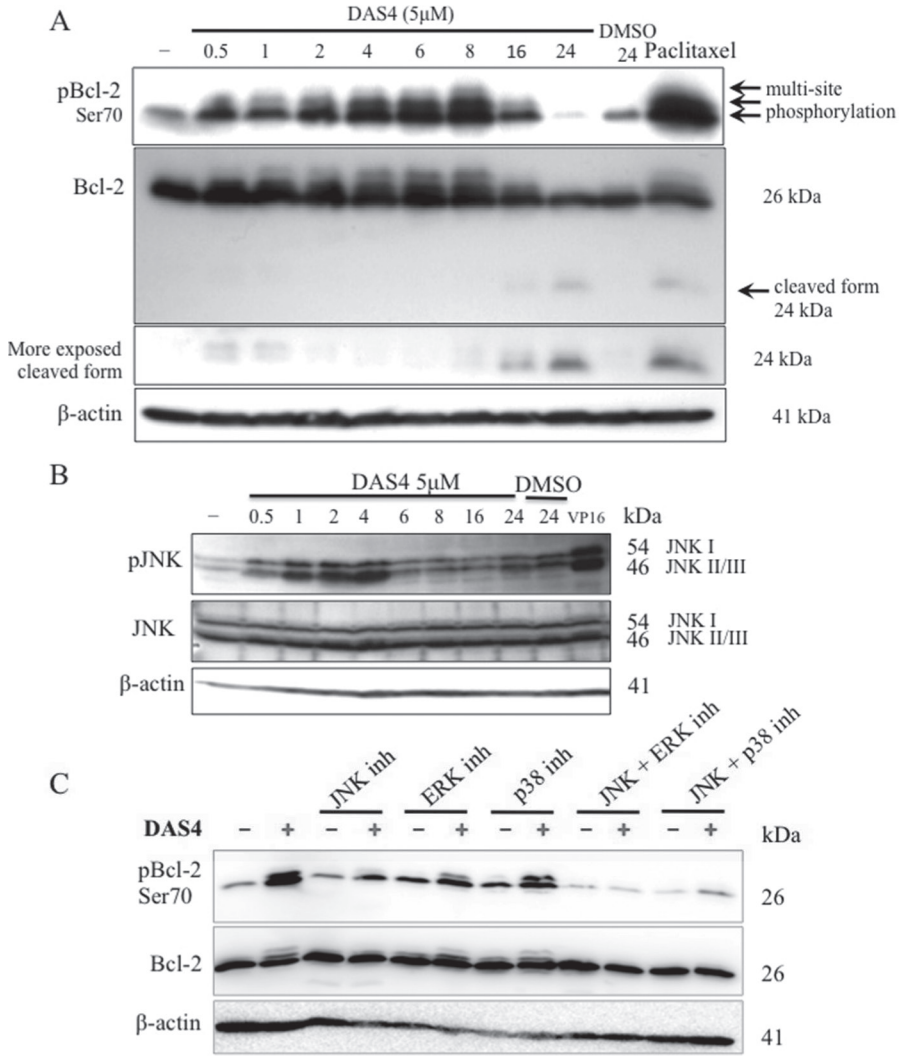

Fig. 3. Bcl-2 multisite phosphorylation occurs prior to its proteolysis and is mediated by JNK. (**A**) Cells were treated with DAS4 (5 μM) and the phosphorylation state of Bcl-2 was investigated after 0.5, 1, 2, 4, 6, 8, 16 and 24 h in comparison with an untreated control (–) and the vehicle (24 h) using an antibody specifically recognizing phospho-Bcl-2 (Ser70). As positive control, the cells were incubated with paclitaxel for 8 h (175 nM). After stripping, the blot was reprobed with anti-Bcl-2 antibody against the complete form of Bcl-2 in order to detect proteolytic bands. β-actin was used as loading control. (**B**) Activation of JNK was examined by analyzing its phosphorylation state. Therefore, the same protein extracts were analyzed by western blotting using anti-phospho-JNK antibody. The signal was compared with that of untreated cells (–) and the vehicle control (24 h DMSO). Protein extracts of cells treated with etoposide (VP16; 100 μM, 2 h) served as positive controls. After stripping, the blot was reprobed with anti-JNK antibody recognizing the complete form. β-actin served as loading control. (**C**) Chemical kinase inhibitors were used to investigate the effect of JNK, ERK and p38MAPK on Bcl-2 multisite phosphorylation. Cells were pre-incubated for 30 min with each kinase inhibitor alone or in combination and then treated for 8 h with DAS4 (5 μM) or vehicle. Cell lysates were analyzed by western blotting using anti-phospho-Bcl-2 (Ser70) and anti-Bcl-2 antibody. β-actin served as loading control.

multisite phosphorylation. NAC prevented the strong phosphorylation of JNK after DAS4 treatment (Figure 5A), whereas JNK remained activated in Trolox pretreated cells (lanes 4 and 6, respectively, compared to line 2).

The analysis of phospho-Bcl-2 (Ser70) antibody revealed that Trolox does not prevent the DAS4-induced multisite phosphorylation of Bcl-2 (see Figure 5B, lanes 2 and 6). No signal was obtained in NAC pretreated cells (line 4). In accordance with our former observation of the specific protective effect of NAC against DAS4-induced cell-cycle arrest and apoptosis, these results demonstrate that NAC likewise inhibited also both the activation of JNK and the multi-site phosphorylation of Bcl-2.

Discussion

We previously identified DAS4 as the most potent inducer of cell death in U937 human lymphoma cells among the tested DASs (10). Caspase-dependent apoptosis was preceded by an early mitotic arrest in prometaphase (10). In the present study, we investigated the exact rationale for the induction of cell-cycle arrest and how this arrest gives way to the onset apoptosis.

In this study, we clearly provided evidence that the biological Activity of DAS4 is ROS-independent. Even if a number of studies have suggested that ROS generation by polysulfides is causative for their biologic effects (12,16,18,52), DAS4 did not raise ROS production at any time in our cell model. Moreover, the ROS scavenger vitamin E analogue Trolox C did not alter the biologic activity of DAS4. Vice versa, the anti-oxidant NAC completely prevented accumulation in G2/M phase and apoptosis, in line with previous findings regarding other polysulfides (18,52). However, NAC may exert its effect even independently on ROS, affecting rather intracellular GSH. As NAC is known to act as pro-GSH molecule augmenting the intracellular pool of reduced GSH and GSH abrogated DAS2-induced mitotic arrest (52), we hypothesized that any increased intracellular small thiols

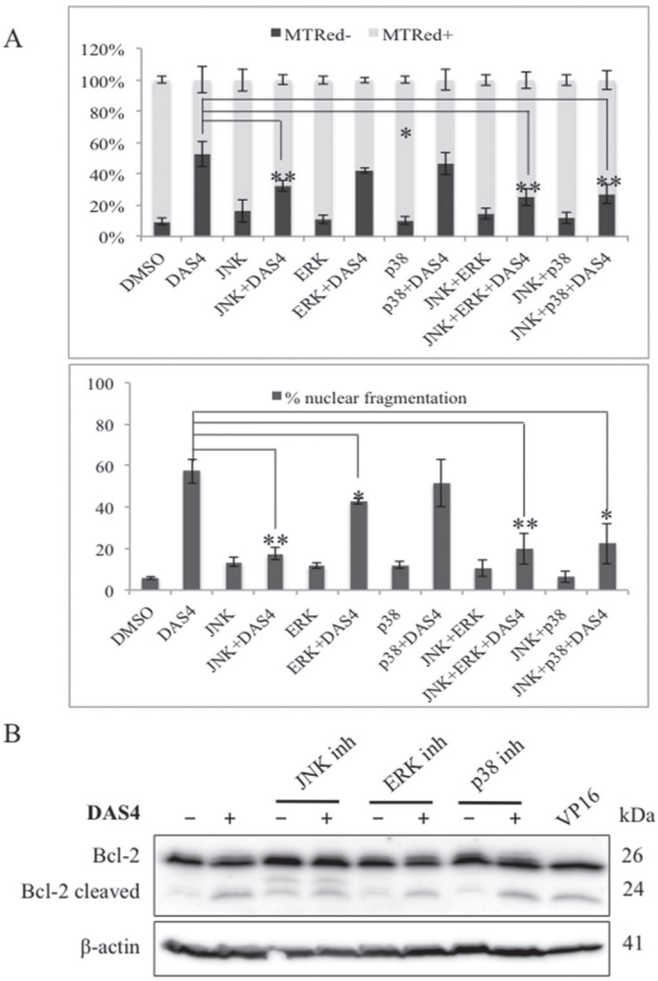

Fig. 4. JNK inhibitor pretreatment significantly decreased DAS4-dependent apoptosis rate and Bcl-2 proteolysis. (**A**) In order to elucidate the effect of kinase inhibitors on apoptosis rate, cells were treated as before (30 min kinase inhibitors followed by 16 h DAS4) and the number of apoptotic cells was quantified either by fluorescence-activated cell sorting following mitotracker red staining (upper panel) or by fluorescence microscopy of Hoechst-stained nuclei (lower panel). The data of three independent experiments are indicated with ±SD and significant changes are highlighted (*<0.05; **<0.01). (**B**) To investigate the effect of the different kinase inhibitors on DAS4-induced Bcl-2 proteolysis, U937 cells were pretreated as before with the different chemical inhibitors of JNK, ERK and p38MAPK. After 16 h incubation with DAS4 (5 μM) protein extracts of U937 cells were analyzed for Bcl-2 proteolysis using western blotting probed with anti-Bcl-2 antibody. Etoposide-treated cells (100 μM, 4 h) served as positive control.

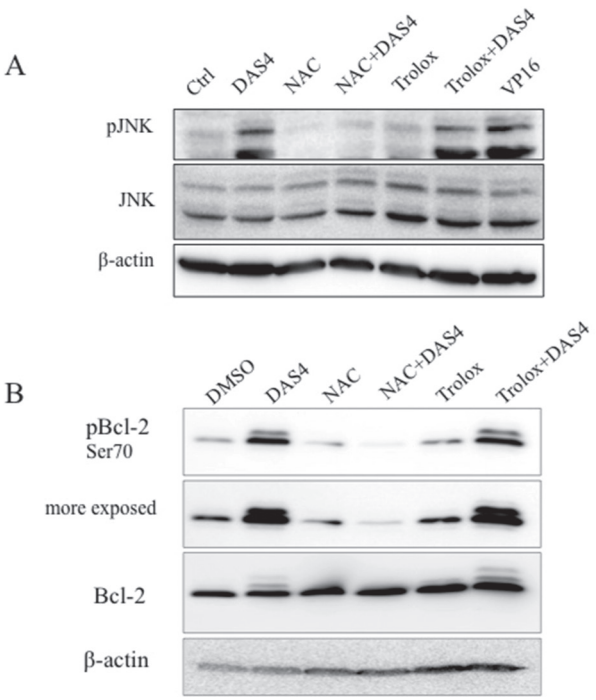

Fig. 5. NAC prevented DAS4-induced JNK activation and multisite phosphorylation of Bcl-2. In order to reveal the power of NAC to interfere with the early JNK activation and JNK-caused Bcl-2 multi-site phosphorylation/proteolysis, western blots were performed. U937 cells were pretreated with the antioxidants NAC or Trolox and subsequently incubated with DAS4. (**A**) After 4 h DAS4 treatment, the resulting protein extracts were separated by sodium dodecyl sulfate–polyacrylamide gel electrophoresis and blotted to a polyvinylidene difluoride membrane. This membrane was probed with phospho-specific JNK antibody, as well as with anti-JNK antibody (after stripping). (**B**) After 8 h of treatment, the cell lysates were used for a western blotting detection with anti-phospo-Bcl-2 and Bcl-2 (after stripping) antibodies.

pool sequestered DAS4, whereas the inability of Trolox to counteract DAS4 results from the missing –SH group. The protective activity of NAC did consequently not arise from its antioxidant nature.

Besides ROS, aberrations during DNA synthesis or disturbances of the microtubule (MT) network might provoke early G2/M arrest (41). DNA damage detected, for example, in response to DAS3 (37) is more likely rooted in early apoptotic steps. As DAS3 and SAMC act at the level of the tubulin network (22,24) and based on our observation that DAS4-treated U937 cells arrested in G2/M lack intact spindle MTs, we proposed that DAS4 likewise might interrupt MT dynamics. Evidence from a tubulin turbidity assay in fact verified the tubulin depolymerizing ability of DAS4 *in vitro*. The inactivity of the long chain carbon analogue of DAS4, 1,9-decadiene, in this assay together with the correlation between tubulin inhibition and the number of sulfur atoms confirmed the key role of sulfur in the interaction with tubulin and excluded hydrophobic interactions as main mode of action [in line with Anwar *et al.* (9)]. The low activity of AM in the *in vitro* assay, which is predicated on its single thiol group, confirmed the importance of sulfur in the interaction between DAS4 and tubulin. Higher polysulfides are reactive toward intracellular (non)protein thiols due to their sulfur–sulfur bonds and might act via thiol–disulfide exchange reactions (9,43). Thus, mass spectrometry analysis of DAS3-treated tubulin revealed that DAS3 directly modifies cysteine residues of β-tubulin under formation of mixed disulfides (22). The fact that the thiol donor NAC (but not Trolox) counteracted DAS4-mediated tubulin depolymerization—even on pure tubulin—strongly supports an occurring thiolation reaction and argues once more against ROS implication. This is in line with a protective role of other sulfhydryl reducing agents (β-mercaptoethanol, DTT) against allicin-induced disruptions of the MT network (53). Such thiol donors probably antagonize cell-cycle arrest and apoptosis by contending with intracellular –SH groups for the interaction with sulfur compounds. Thiol–disulfide exchange reactions are in general expected to be reversible due to an adequate cellular GSH level (43). However, like other OSCs, DAS4 partially depleted the intracellular GSH content. As GSH is quite abundant in cells, it is likely to be targeted by DAS4. The resulting GSH-DAS4 adducts might be extruded from the cell similar to GSSG, thus explaining the irreversible modulation of the MT network. Due to the abundance of tubulin within the cell and the adjacency of the MTs plus ends to the cellular membrane as entry site of DAS4, together with the importance of the mitotic spindle assembly during mitosis, tubulin most likely represents the major cellular target of DAS4. Besides, we did not detect any consistent DNA damage during the time of DAS4-treatment determining mitotic arrest, thus excluding this latter event as an early causative event for DAS4 effects on cell cycle and apoptosis. As a consequence

of tubulin disarrangements, the formation of proper spindle microtubules fails activating the mitotic spindle assembly checkpoint and inducing early mitotic arrest. How this mitotic arrest finally ends in apoptosis was not elucidated yet. Here, we prove that multisite phosphorylation of Bcl-2 caused by DAS4-mediated microtubule disorganization may evoke its proteolysis and finally links mitotic arrest to the onset of apoptosis. We have documented a very early multisite phosphorylation of Bcl-2 protein involving also Ser70 upon DAS4 treatment. In contrast to single-site phosphorylation occurring during normal cell-cycle progression (27), a multisite phosphorylation (at Ser70, Ser87 and Thr69), observed for other antimitotic agents, rather converts the prosurvival activity of Bcl-2 into a pro-apoptotic function (28,30,31). Strikingly, this modification coincided with the maximal accumulation of U937 cells in early mitosis and preceded the appearance of apoptotic cells (10). This timing suggests that multisite phosphorylation of Bcl-2 is requisite for its proteolysis, which takes place at later times (10). U937 cells express high Bcl-2 protein levels; strategies aiming at impairing Bcl-2 expression/activity are able per se to trigger apoptosis in this cellular model (50). Accordingly our results are in favor of a Bcl-2 addiction developed by these cells. Nevertheless, the percentage of apoptotic cells is significantly reduced in combinational treatments with DAS4 and a small molecule Bcl-2 inhibitor compared with the sum of the effects produced by the single treatments. No impact on cell cycle is observed, supporting a pro-apoptotic role of Bcl-2 downregulation only downstream of cell-cycle arrest. Of interest, this event occurs in fact simultaneously with the massive DAS4-dependent activation of Bax and caspase-3 activity (10). The elevated level of Bcl-2 protein expression in U937 cells suggests a possible marker of susceptibility of cancer cells to sulfur compounds and prompts to verify this assumption in cells expressing Bcl-2 at different levels in future studies.

Next, we aimed at identifying the upstream kinase(s) and our data revealed that JNK may act as intermediate transducer of DAS4-mediated stress (10) via Bcl-2 protein modification. We witnessed an early and transient JNK phosphorylation following DAS4 treatment. Remarkably, the timing (0.5–4 h) coincides with tubulin depolymerization and Bcl-2 phosphorylation. Beyond, the role of JNK was proven by the chemical JNK inhibitor SP600125, which entirely prevented Bcl-2 multisite phosphorylation. In line with previous data, ERK inhibitor partially protected Bcl-2 from this posttranslational modification, whereas p38 was not involved at all (54). The implication of JNK was not completely unexpected as a causal relationship between garlic-derived OSCs and JNK activation was observed in various cancer cell lines (16,22,24,49,54,55) and JNK has been suggested to mediate Bcl-2 phosphorylation in response to changes of the MT network (56,57). We did not only show that JNK-mediated multisite phosphorylation of Bcl-2 is causative for its proteolysis but further provided evidence that the latter might trigger apoptosis. Similar to DAS3-induced apoptosis of prostate cancer and adenocarcinoma cells (24,38), pharmacological JNK inhibition in fact protected DAS4-treated U937 cells significantly from apoptosis and likewise affected Bcl-2 cleavage. ERK plays a minor role in this process, possibly acting downstream or as part of an amplification loop while the activity of p38 MAPK was not relevant. As ASK1 and JNK1 are activated at G2/M phase during normal cell-cycle progression and phosphorylate Bcl-2 *in vivo* (28), this modulation might represent a normal physiological process, which is simply amplified due to sustained JNK activation during a persisting mitotic arrest (48). Bcl-2 phosphorylation may thus be part of a sensing system of MT integrity and represent a way to prepare mitotic cells for their future elimination if the formation of proper spindle MTs fails (48). JNK appears implicated in DAS4-mediated effects on Bcl-2 and apoptosis. How JNK is activated remains a point to be addressed. Here, we may attempt some speculations. We have observed that JNK activation occurs very early upon DAS4 treatment (within 0.5 h). An early activation of JNK is specifically described for MT inhibitors (58). Our results strongly suggest the existence of a common earlier event triggered by MT disruption. Canonically, a number of MAPKKKs activate JNK. Although we cannot exclude that the redox disequilibrium induced by DAS4 at early time points may play a role in activating specific

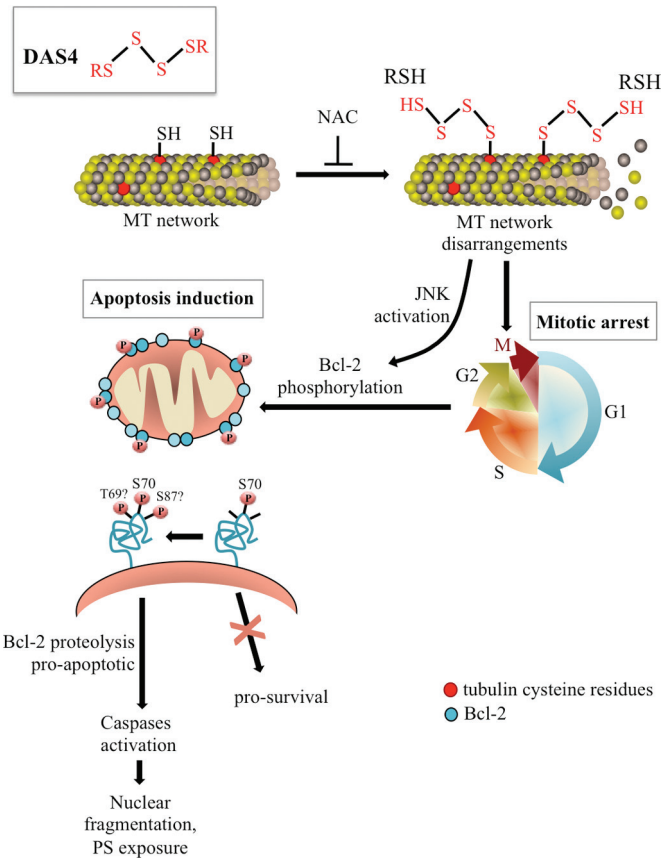

Fig. 6. Model of the mode of action of DAS4. Based on our data obtained throughout this study, we propose a model of the mode of action of DAS4. First, this organosulfur compound directly interacts via its sulfur atoms with cysteine residues of target proteins. The interaction between DAS4 and tubulin as major cellular target occurs within minutes and causes disarrangements of the MT network. Due to the inability of the cell to form correct spindle MTs, the mitotic spindle assembly checkpoint is activated and leads to cell-cycle arrest at G2/M phase detectable at 4 h with peak at 8 h. After prolonged mitotic arrest, cells undergo apoptosis via the intrinsic pathway. The early activation of JNK is concomitant with the multisite phosphorylation of the anti-apoptotic protein Bcl-2. Prevention of this Bcl-2 modification, as well as subsequent proteolytic cleavage and apoptosis in cells pre-treated with a chemical JNK-inhibitor, leads us the assumption that this kinase together with the JNK-dependent Bcl-2 multisite phosphorylation of Bcl-2 represent the missing link between DAS4-induced mitotic arrest and the onset of apoptosis.

redox-sensitive MAPKKKs [i.e. ASK-1 (59)] operating upstream to JNK, there is no clear-cut evidence, however, that other MT inhibitors do act via similar early modulations. Interestingly, there is evidence that JNK itself is associated with MT components (60); moreover, MAPKKKs co-localize with activated JNK along MT network (60). These findings suggest that MAPKKKs and JNK may be physiological components of the MT scaffold. Some MAPKKKs upstream to JNK (or JNK itself?) could be activated by a forced MT remodeling [a similar event has been suggested to occur under mechanical stress (61)] and subsequently could co-ordinate a stress response. This model implies that JNK activation might play a role even very upstream, in controlling the progression of mitosis. For example, JNK has been shown to act upstream of aurora B kinase (62), which directly mediates phosphorylation of histone H3 at serine 10 (63).

The ability of NAC to completely inhibit JNK activation and subsequent Bcl-2 multisite phosphorylation strengthens the causality between active JNK and this pro-apoptotic modification of Bcl-2. It further substantiates that both events are directly induced by thiol–disulfide exchange reactions of DAS4 with cellular target(s).

This study revealed a clear, logical time course of events mediated by DAS4 (Figure 6). Within the first minutes, DAS4 binds via thiolation to tubulin and impairs MT dynamic, thereby disturbing the assembly of correct mitotic spindle. Tubulin depolymerization then activates JNK within the first 30 min, which mediates multisite phosphorylation of the anti-apoptotic protein Bcl-2. This modulation peaks with G2/M arrest at 8 h and gives way to Bcl-2 proteolysis and thus finally induces apoptosis. Bcl-2 cleavage might cause the liberation of the pro-apoptotic member Bax, which is now able to massively trigger apoptosis via the complete release of apoptotic factors from mitochondria.

Supplementary data

Supplementary Figures 1-3 can be found at http://carcin.oxfordjournals.org/

Funding

Fonds National de la Recherche Luxembourg to M.K.; Action Lions "Vaincre le Cancer" to C.C; Recherche Cancer et Sang foundation, Recherches Scientifiques Luxembourg association, EenHaerz fir kriibskrank Kanner association, the Action Lions Vaincre le Cancer association and Télévie Luxembourg to Research at the Laboratoire de Biologie Moléculaire et Cellulaire du Cancer; University of Saarland, the Ministry of Economics and Science of Saarland, the Deutsche Forschungsgemeinschaft (JA1741/2-1) and the European Union (ITN "RedCat" 215009, Interreg IVa project "Corena")

Acknowledgements

The authors thank the Foundation for Scientific Cooperation between Germany and Luxemburg for additional support.

Conflict of Interest Statement: None declared.

References

1. Powolny,A.A. *et al.* (2008) Multitargeted prevention and therapy of cancer by diallyl trisulfide and related Allium vegetable-derived organosulfur compounds. *Cancer Lett.*, **269**, 305–314.
2. Shukla,Y. *et al.* (2007) Cancer chemoprevention with garlic and its constituents. *Cancer Lett.*, **247**, 167–181.
3. Gonzalez,C.A. *et al.* (2006) Fruit and vegetable intake and the risk of stomach and oesophagus adenocarcinoma in the European Prospective Investigation into Cancer and Nutrition (EPIC-EURGAST). *Int. J. Cancer*, **118**, 2559–2566.
4. Hsing,A.W. *et al.* (2002) Allium vegetables and risk of prostate cancer: a population-based study. *J. Nat. Cancer Inst.*, **94**, 1648–1651.
5. Scherer,C. *et al.* (2009) Potential role of organic sulfur compounds from Allium species in cancer prevention and therapy. *Phytochem Rev.*, **8**, 349–368.
6. Wargovich,M.J. (2001) Colon cancer chemoprevention with ginseng and other botanicals. *J. Korean Med. Sci.*, **16**, S81–S86.
7. Cerella,C. *et al.* (2011) Chemical properties and mechanisms determining the anti-cancer action of garlic-derived organic sulfur compounds. *Anticancer Agents Med. Chem.*, **11**, 267–271.
8. Cerella,C. *et al.* (2011) Naturally occurring organic sulfur compounds: an example of a multitasking class of phytochemicals in anti-cancer research. In Rasooli, I. (Ed.) *Anti-Cancer Research, Phytochemicals - Bioactivities and Impact on Health*. **Vol. 2**. InTech, Rijeka, Croatia, pp. 1–40.
9. Anwar,A. *et al.* (2008) Naturally occurring reactive sulfur species, their activity against Caco-2 cells, and possible modes of biochemical action. *J. Sulphur Chem.*, **29**, 251–268.
10. Cerella,C. *et al.* (2009) Cell cycle arrest in early mitosis and induction of caspase-dependent apoptosis in U937 cells by diallyltetrasulfide (Al2S4). *Apoptosis*, **14**, 641–654.
11. Fukao,T. *et al.* (2004) The effects of allyl sulfides on the induction of phase II detoxification enzymes and liver injury by carbon tetrachloride. *Food Chem. Toxicol*, **42**, 743–749.
12. Jakubikova,J. *et al.* (2006) Garlic-derived organosulfides induce cytotoxicity, apoptosis, cell cycle arrest and oxidative stress in human colon carcinoma cell lines. *Neoplasma*, **53**, 191–199.
13. Busch,C. *et al.* (2010) Diallylpolysulfides induce growth arrest and apoptosis. *Int. J. Oncol*, **36**, 743–749.
14. Viry,E. *et al.* (2011) Antiproliferative effect of natural tetrasulfides in human breast cancer cells is mediated through the inhibition of the cell division cycle 25 phosphatases. *Int. J. Oncol.*, **38**, 1103–1111.
15. Antosiewicz,J. *et al.* (2006) c-Jun NH(2)-terminal kinase signaling axis regulates diallyl trisulfide-induced generation of reactive oxygen species and cell cycle arrest in human prostate cancer cells. *Cancer Res.*, **66**, 5379–5386.
16. Filomeni,G. *et al.* (2003) Reactive oxygen species-dependent c-Jun NH2-terminal kinase/c-Jun signaling cascade mediates neuroblastoma cell death induced by diallyl disulfide. *Cancer Res.*, **63**, 5940–5949.
17. Kim,Y.A. *et al.* (2007) Mitochondria-mediated apoptosis by diallyl trisulfide in human prostate cancer cells is associated with generation of reactive oxygen species and regulated by Bax/Bak. *Mol. Cancer. Ther.*, **6**, 1599–1609.
18. Xiao,D. *et al.* (2005) Diallyl trisulfide-induced G(2)-M phase cell cycle arrest in human prostate cancer cells is caused by reactive oxygen species-dependent destruction and hyperphosphorylation of Cdc 25 C. *Oncogene*, **24**, 6256–6268.
19. Yang,J.S. *et al.* (2009) Diallyl disulfide induces apoptosis in human colon cancer cell line (COLO 205) through the induction of reactive oxygen species, endoplasmic reticulum stress, caspases casade and mitochondrial-dependent pathways. *Food Chem. Toxicol.*, **47**, 171–179.
20. Yi,L. *et al.* (2010) Diallyl disulfide induces apoptosis in human leukemia HL-60 cells through activation of JNK mediated by reactive oxygen. *Die. Pharmazie.*, **65**, 693–698.
21. Panayiotidis, M. (2008) Reactive oxygen species (ROS) in multistage carcinogenesis. *Cancer Lett.*, **266**, 3–5.
22. Hosono,T. *et al.* (2005) Diallyl trisulfide suppresses the proliferation and induces apoptosis of human colon cancer cells through oxidative modification of beta-tubulin. *J. Biol. Chem.*, **280**, 41487–41493.
23. Hosono,T. *et al.* (2008) Alkenyl group is responsible for the disruption of microtubule network formation in human colon cancer cell line HT-29 cells. *Carcinogenesis*, **29**, 1400–1406.
24. Xiao,D. *et al.* (2003) Induction of apoptosis by the garlic-derived compound S-allylmercaptocysteine (SAMC) is associated with microtubule depolymerization and c-Jun NH(2)-terminal kinase 1 activation. *Cancer Res.*, **63**, 6825–6837.
25. Ghibelli,L. *et al.* (2010) Multistep and multitask Bax activation. *Mitochondrion*, **10**, 604–613.
26. Ito,T. *et al.* (1997) Bcl-2 phosphorylation required for anti-apoptosis function. *J. Biol. Chem.*, **272**, 11671–11673.
27. Ruvolo,P.P. *et al.* (2001) Phosphorylation of Bcl2 and regulation of apoptosis. *Leukemia*, **15**, 515–522.
28. Yamamoto,K. *et al.* (1999) BCL-2 is phosphorylated and inactivated by an ASK1/Jun N-terminal protein kinase pathway normally activated at G(2)/M. *Mol. Cell. Biol.*, **19**, 8469–8478.
29. Basu,A. *et al.* (1998) Microtubule-damaging drugs triggered bcl2 phosphorylation-requirement of phosphorylation on both serine-70 and serine-87 residues of bcl2 protein. *Int. J. Oncol.*, **13**, 659–664.
30. Haldar,S. *et al.* (1995) Inactivation of Bcl-2 by phosphorylation. *Proc. Natl. Acad. Sci. U. S. A.*, **92**, 4507–4511.
31. Haldar,S. *et al.* (1996) Taxol induces bcl-2 phosphorylation and death of prostate cancer cells. *Cancer Res.*, **56**, 1253–1255.
32. Derbesy,G. *et al.* (1994) A simple method to prepare unsymmetrical di- tri- and tetrasulfides. *Tetrahedron Lett.*, **35**, 5381–5384.
33. Milligan,B. *et al.* (1961) New syntheses of trisulphides. *J. Chem. Soc.*, 4850–4853.
34. Schneider,T. *et al.* (2011) Interactions of polysulfanes with components of red blood cells. *Med. Chem. Comm.*, **2**, 196–200.
35. Juncker,T. *et al.* (2011) UNBS1450, a steroid cardiac glycoside inducing apoptotic cell death in human leukemia cells. *Biochem. Pharmacol.*, **81**, 13–23.
36. Schumacher,M. *et al.* (2010) Heteronemin, a spongean sesterterpene, inhibits TNF alpha-induced NF-kappa B activation through proteasome inhibition and induces apoptotic cell death. *Biochem. Pharmacol.*, **79**, 610–622.
37. Wang,H.C. *et al.* (2010) Allyl sulfides inhibit cell growth of skin cancer cells through induction of DNA damage mediated G2/M arrest and apoptosis. *J. Agric. Food Chem.*, **58**, 7096–7103.
38. Wu,X.J. *et al.* (2009) Apoptosis induction in human lung adenocarcinoma cells by oil-soluble allyl sulfides: triggers, pathways, and modulators. *Environ. Mol. Mutagen.*, **50**, 266–275.
39. Dickinson,D.A. *et al.* (2002) Cellular glutathione and thiols metabolism. *Biochem. Pharmacol.*, **64**, 1019–1026.
40. Cerella,C. *et al.* (2011) COX-2 inhibitors block chemotherapeutic agent-induced apoptosis prior to commitment in hematopoietic cancer cells. *Biochem. Pharmacol.*, **82**, 1277–1290.

41. Singh,P. *et al.* (2008) Microtubule assembly dynamics: an attractive target for anticancer drugs. *IUBMB life*, **60**, 368–375.
42. Karr,T.L. *et al.* (1980) Calcium ion induces endwise depolymerization of bovine brain microtubules. *J. Biol. Chem.*, **255**, 11853–11856.
43. Munchberg,U. *et al.* (2007) Polysulfides as biologically active ingredients of garlic. *Org. Biomol. Chem.*, **5**, 1505–1518.
44. Wang,T.H. *et al.* (1998) Microtubule-interfering agents activate c-Jun N-terminal kinase/stress-activated protein kinase through both Ras and apoptosis signal-regulating kinase pathways. *J. Biol. Chem.*, **273**, 4928–4936.
45. Mhaidat,N.M. *et al.* (2007) Docetaxel-induced apoptosis of human melanoma is mediated by activation of c-Jun NH2-terminal kinase and inhibited by the mitogen-activated protein kinase extracellular signal-regulated kinase 1/2 pathway. *Clin. Cancer Res.*, **13**, 1308–1314.
46. Wang,T.H. *et al.* (1999) Microtubule dysfunction induced by paclitaxel initiates apoptosis through both c-Jun N-terminal kinase (JNK)-dependent and -independent pathways in ovarian cancer cells. *J. Biol. Chem.*, **274**, 8208–8216.
47. Lee,L.F. *et al.* (1998) Paclitaxel (Taxol)-induced gene expression and cell death are both mediated by the activation of c-Jun NH2-terminal kinase (JNK/SAPK). *J. Biol. Chem.*, **273**, 28253–28260.
48. Fan,M. *et al.* (2000) Modulation of mitogen-activated protein kinases and phosphorylation of Bcl-2 by vinblastine represent persistent forms of normal fluctuations at G2-M1. *Cancer Res.*, **60**, 6403–6407.
49. Lei,X.Y. *et al.* (2008) Apoptosis induced by diallyl disulfide in human breast cancer cell line MCF-7. *Acta Pharmacol. Sin.*, **29**, 1233–1239.
50. Radogna,F. *et al.* (2007) Melatonin antagonizes apoptosis via receptor interaction in U937 monocytic cells. *J. Pineal Res.*, **43**, 154–162.
51. Enyedy,I.J. *et al.* (2001) Discovery of small-molecule inhibitors of Bcl-2 through structure-based computer screening. *J. Med. Chem.*, **44**, 4313–4324.
52. Song,J.D. *et al.* (2009) Molecular mechanism of diallyl disulfide in cell cycle arrest and apoptosis in HCT-116 colon cancer cells. *J. Biochem. Mol. Toxicol.*, **23**, 71–79.
53. Prager-Khoutorsky,M. *et al.* (2007) Allicin inhibits cell polarization, migration and division via its direct effect on microtubules. *Cell Motil. Cytoskeleton*, **64**, 321–337.
54. Xiao,D. *et al.* (2004) Diallyl trisulfide-induced apoptosis in human prostate cancer cells involves c-Jun N-terminal kinase and extracellular-signal regulated kinase-mediated phosphorylation of Bcl-2. *Oncogene*, **23**, 5594–5606.
55. Lee,B.C. *et al.* (2011) Role of Bim in diallyl trisulfide-induced cytotoxicity in human cancer cells. *J. Cell. Biochem.*, **112**, 118–127.
56. Basu,A. *et al.* (2003) Identification of a novel Bcl-xL phosphorylation site regulating the sensitivity of taxol- or 2-methoxyestradiol-induced apoptosis. *FEBS Lett.*, **538**, 41–47.
57. Chen,J. *et al.* (2008) Microtubule depolymerization and phosphorylation of c-Jun N-terminal kinase-1 and p38 were involved in gambogic acid induced cell cycle arrest and apoptosis in human breast carcinoma MCF-7 cells. *Life Sci.*, **83**, 103–109.
58. Stone,A.A. *et al.* (2000) Microtubule inhibitors elicit differential effects on MAP kinase (JNK, ERK, and p38) signaling pathways in human KB-3 carcinoma cells. *Exp. Cell Res.*, **254**, 110–119.
59. Ueda,S. *et al.* (2002) Redox control of cell death. *Antioxid. Redox Signal.*, **4**, 405–414.
60. Nagata,K. *et al.* (1998) The MAP kinase kinase kinase MLK2 co-localizes with activated JNK along microtubules and associates with kinesin superfamily motor KIF3. *EMBO J.*, **17**, 149–158.
61. Pereira,A.M. *et al.* (2011) Integrin-dependent activation of the JNK signaling pathway by mechanical stress. *PloS one*, **6**, e26182.
62. Oktay,K. *et al.* (2008) The c-Jun N-terminal kinase JNK functions upstream of Aurora B to promote entry into mitosis. *Cell Cycle*, **7**, 533–541.
63. Hirota,T. *et al.* (2005) Histone H3 serine 10 phosphorylation by Aurora B causes HP1 dissociation from heterochromatin. *Nature*, **438**, 1176–1180.

Received January 9, 2012; revised June 10, 2012; accepted July 3, 2012